CANYON DIABLO METEORITE: METALLOGRAPHIC AND MASS SPECTROMETRIC STUDY OF 56 FRAGMENTS

DIETER HEYMANN
MICHAEL E. LIPSCHUTZ
BETTY NIELSON
AND
EDWARD ANDERS

A Reprint from

JANUARY 15, 1966

Journal of Geophysical Research

VOLUME 71 NUMBER 2

PUBLISHED BY
THE AMERICAN GEOPHYSICAL UNION

Canyon Diablo Meteorite: Metallographic and Mass Spectrometric Study of 56 Fragments

DIETER HEYMANN

Enrico Fermi Institute for Nuclear Studies
University of Chicago, Chicago, Illinois

MICHAEL E. LIPSCHUTZ[1]

Physikalisches Institut
Universität Bern, Berne, Switzerland

BETTY NIELSEN AND EDWARD ANDERS

Enrico Fermi Institute for Nuclear Studies
University of Chicago, Chicago, Illinois

Abstract. In an attempt to reconstruct the history of the surviving Canyon Diablo fragments, we have studied 56 specimens by metallography and mass spectrometry and 5 others by metallography only. Of these, 25 came from the rim of the crater, and 36 from the plains. Fifteen contained diamonds. On the basis of metallographically observable reheating effects, the samples were classified as strongly, moderately, and lightly shocked, corresponding to shock pressures of $\geq$750 kb, 130–750 kb, and $<$130 kb. The division among these categories was as follows. Plains: 0, 14, and 86%; rim: 72, 28, and 0%; diamond-bearing: 67, 33, and 0%. This bears out earlier observations by Nininger and the authors that rim (and diamond-bearing) specimens tend to be much more strongly reheated than plains specimens. To determine the original depth in the meteoroid from which the specimens came, we measured their He^3 content. The values vary by a factor of 10^4, ranging from $\leq 0.03 \times 10^{-8}$ to 294×10^{-8} cc STP/g He^3. Apparently, the great majority of samples come from the outermost 2 of the meteoroid. There appears to be a distinct grading of shock effects with depth; the mean depth of the lightly shocked specimens is 72 cm, whereas that of the moderately and strongly shocked specimens is 132 cm. Diamond-bearing and rim specimens also come from greater mean depths: 135 and 127 cm, in contrast to the depth of the plains specimens (81 cm). The moderately to strongly shocked specimens, as well as the metallic spherules resulting from the vaporization of the meteorite, show a marked localization northeast and southeast of the crater. The throwout pattern for shocked material seems to have been highly directional, like the lunar ray craters. Measurements of He, Ne, and Ar in 14 of the most gas-rich samples gave a cosmic-ray age of 540 m.y. for 7 and 170 m.y. for 5 samples. The Canyon Diablo object apparently originated in a breakup 540 m.y. ago and suffered a secondary collision in space 170 m.y. ago.

1. INTRODUCTION

Barringer's 1909 paper, in which he proposed an impact origin of Meteor Crater, Arizona, contains a map showing the distribution of Canyon Diablo meteorites around the crater. Many small specimens (usually $\leq$5 kg in weight) were concentrated on the northeast rim of the crater; others, ranging up to 500 kg in weight, were scattered over the surrounding plains, at distances of up to 9 km from the crater. *Nininger* [1950, 1956] later drew attention to some remarkable differences between these two populations. The 'rim' specimens (from both the northeast and southeast parts of the rim) nearly always showed evidence of reheating to $\geq$760°C and often contained diamonds. The 'plains' specimens, on the other hand, were not reheated and did not contain diamonds. Later we established that the reheating had apparently lasted for only a few seconds and had been followed by a rapid quench [*Lip-*

[1] Now at the Department of Chemistry, Purdue University, Lafayette, Indiana.

schutz and Anders, 1961*a*]. These observations led to the suggestion that the diamonds were produced by the impact shock [*Nininger,* 1956; *Lipschutz and Anders,* 1961*a, b*].

It was not known, however, how these striking differences between rim and plains populations were related to their positions in the original meteoroid. Fortunately, this problem can be attacked experimentally. In a meteoroid exposed to cosmic rays in space, the production rate of a cosmogenic nuclide such as He^3 decreases nearly exponentially with increasing depth [*Signer and Nier,* 1960; *Arnold et al.,* 1961]. Hence the concentration of He^3 indicates the original distance of a sample from the preatmospheric surface, provided that all parts of the meteoroid were irradiated for the same length of time.

For the present study, we obtained from Nininger 45 Canyon Diablo specimens whose locations with respect to the crater were known (samples 1–45, Table 1). Twelve of these were rim specimens, from either the northeast or the southeast rim. The remaining 33 were plains

TABLE 1. Summary of Experimental Results

No.	Nininger No.[a]	Location[b] (Sec. No.)	Weight, g	Shock and Reheating Symptoms[c]					Class[d]	He^{3e} 10^{-8} cc STP/g
				ϵFe	KRx	Cdiff	FeS	Eu		
1	4328	16	640				1		G	*3.9*
2	4329	16	625	+	(+)				M	*≤0.1*
3	4330	16	569	+	+				M	≤0.1
4	4302	18	2551							*0.3*
5	4811	28	357	+	+		2		MD	*0.3*
6	4812	28	557							0.3
7	4813	28	1201							109
8	4437	30	770							3.8
9	4442	30	1278						G	*1.9*
10	4335	32	314	+	+	m+			M	≤0.07
11	4337	32	1660				1			**21.9**
12	4323	6	595				1			0.7
13	4325	6	1047						G	174
14	4326	6	136							31
15	2654	13, NE Rim	777		++	p++			H	*0.23*
16	2659	13, NE Rim	366		++	m++, p++		L, Ph	H	≤0.1
17	2660	13, NE Rim	622		++	m++, p++	2, 3	L, Ph	HD	≤0.06
18	2727	13, NE Rim	652		++	p++			H	*0.7*
19	2730	13, NE Rim	213		++	p++		Ph+	H	1.6
20	2739	13, NE Rim	221	+	(+)				M	65.5
21	3744	14	336							≤0.2
22	4339	14	657							*2.4*
23	4340	14	554							46.8
24	4341	14	448						G	**294**
25	4441	20	951							*0.8*
26	4814	21	966							**36.2**
27	4344	22	638							**12.2**
28	4345	22	329	+	(+)				M	*2.3*
29	4347	22	262							*0.6*
30	2840	24, SE Rim	668		++	p++	2, 3	L, Ph	HD	*3.0*
31	2842	24, SE Rim	554		++	m+		L, Ph	H	*≤0.03*
32	2843	24, SE Rim	535		++	p+			H	*0.2*
33	2845	24, SE Rim	511		++	p+, m+			H	0.3
34	2851	24, SE Rim	423		++	m++		L, Ph	H	*1.9*
35	2855	24, SE Rim	362	+	+				M	*≤0.16*
36	3740	26	2253							*0.7*
37	4366	34	44							0.3
38	4367	34	88							109
39	4368	34	189							17
40	4369	34	280							≤0.1

TABLE 1. (Continued)

No.	Nininger No.[a]	Location[b] (Sec. No.)	Weight, g	Shock and Reheating Symptoms[c]					Class[d]	He^{3}[e] 10^{-8} cc STP/g
				ϵFe	KRx	Cdiff	FeS	Eu		
41	4727	34	441							*0.6*
42	4733	34	434							*4.9*
43	4352	36	370							**33.6**
44	4353	36	543							**14.7**
45	4354	36	467							*0.3*
46	4719	Rim	185		++	m++	3		HD	0.8
47	4721[f]	Rim?	198	+	+				M	35.2
48	4722	Rim			++	m++	3	Ph	HD	0.15
49	2755	Rim			++	m++	2, 3	L, Ph	HD	8.3
50	—[a]	Rim	>150		++	p+	3	L, Ph	HD	0.9
51	—[a, g]	Rim	>2000		+	?	?	?	MD?	≤0.1
52	—[a]	Rim	>412	+	+	m+	2, 3	L	MD	0.26
53	2758	Rim			++	m++	3	L, Ph	HD	5.1
54A	—[a, h]	?								33.1
54C	—[a, h]	Rim?		+	(+)		1, 2		MD	*0.18*
55	4703	Rim			++	m++	2, 3	L, Ph	HD	1.1
56	4729	Rim			++	m++	2, 3	L, Ph	HD	0.8
57	4041.2	Rim			++	m++, p++	2, 3	L, Ph	HD	
58	4043.2	Rim		+	+		2, 3		MD	
59	4012.2	Plains					1			
60	4047.2	Plains					1			
61	4050.2	Plains					1			

[a] All of Nininger's Canyon Diablo specimens carry the prefix number 34, in addition to the 4-digit number listed. The remaining specimens are: No. 50, sample 1 from *Lipschutz and Anders* [1961*a*]; Nos. 51 and 52, samples 2262 and 1724 from the U. S. National Museum. The latter was previously described by *Nininger* [1939], *Ksanda and Henderson* [1939], and *Lipschutz and Anders* [1961a]. Numbers 54A and 54C are reported to be portions of *Carter and Kennedy's* [1964] sample No. 3. Numbers 57 to 61 were obtained from the Nininger collection through the courtesy of Carleton B. Moore of Arizona State University. They were described as 'rim' or 'plains,' but their exact location was not known.

[b] Full location data are: Township 19N, Range 13E: Sections 16, 18, 28, 30, 32, and 6; Township 19N, Range 12 1/2 E: Sections 13, 14, 20, 21, 22, 24, 26, 34, 36.

[c] *Headings*: ϵFe, ϵ-iron transformation structure; KRx, recrystallized kamacite; Cdiff, carbon diffusion zone; FeS, troilite; Eu, phosphide and carbide eutectics. *Symbols*: (+), feature seen only along fault lines and phase boundaries; +, feature seen in localized areas; ++, feature seen throughout specimen; m, martensite; p, pearlite; 1, 2, 3, polycrystalline or remelted troilite, as defined in section 2; L, ledeburite-like eutectic; Ph, phosphide eutectics.

[d] M, moderately shocked (130–750 kb); H, heavily shocked (≥750 kb); D, diamond; G, cohenite graphitized in cracks, either due to weathering or sustained reheating by hot ejecta.

[e] Values printed in italics are single measurements. Samples known to have cosmic-ray ages other than 540 m. y. are printed in boldface type. For the purpose of Figure 10, their He^{3} contents were recalculated to 540 m. y.

[f] This sample was stored with the rim specimens in the American Meteorite Museum, but its original location was not recorded at the time of collection and was therefore not known with certainty. It was reported to contain numerous small diamonds, but we found none after repolishing. This sample may be a piece of Canyon Diablo 2, since it is a medium, rather than a coarse, octahedrite.

[g] This meteorite contained a large diamond, about 1 mm in diameter, at the center of the slice. The surface was rough and badly gouged, and the troilite portions were deeply recessed. To repolish this specimen, it would have been necessary to remove the diamond, which was not permitted under the terms of the loan. We were therefore unable to repolish more than a small corner of it. The kamacite was completely recrystallized, but, since we had no positive evidence that this was the case throughout the remainder of the slice, we recorded a single + in the KRx column and classified this sample as moderately shocked.

[h] Both samples allegedly came from the same 15-cm specimen, but the He^{3} contents, differing by a factor of 180, imply that they were separated by a distance of at least 110 cm. The shock effects also differ quite drastically. Only 54C matches the Carter and Kennedy No. 3 specimen morphologically, and the origin of 54A is therefore in doubt [*Anders and Lipschutz*, 1965].

specimens, representing 13 of the 1-mile (1609 m) surveyor's sections in the crater area. Their exact location within each square was not known, except for samples 8 and 9 which came from the southeast part of the section. In addition, we obtained from various sources 11 specimens known or believed to contain diamonds (samples 46–56). All but one had originally been collected by Nininger, and, since he states that he found diamond-bearing samples only on the rim, we have listed these samples as rim specimens. In several cases where the identification of the diamonds seemed uncertain, we checked them by X-ray diffraction. In one sample (no. 47), the presumed diamonds disappeared during repolishing, before they could be X-rayed. Various observations make it unlikely that they were diamonds. To improve our statistics on troilite-bearing samples, we obtained five such specimens (nos. 57–61) from Carleton B. Moore of Arizona State University. These samples were received toward the end of our survey and were studied only metallographically. Two of these were rim specimens and contained diamonds. Counting the six troilite and three diamond inclusions discovered during this study, the following breakdown of samples resulted:

Rim	25
Plains	36
Diamond-bearing	15
Troilite-bearing	20

Location data for all samples are given in Table 1. Each sample was studied by metallographic techniques to determine its temperature history. The He^3 content was measured on a mass spectrometer. In twelve samples where the noble-gas content was high enough, neon and argon were measured also. These data (and two earlier measurements [*Heymann,* 1964]) were used in calculating the cosmic ray exposure age of Canyon Diablo.

2. Experimental Procedure

Temperature and Pressure History

Öpik [1958] pointed out several years ago that the surviving Canyon Diablo fragments presumably came from the rear part of the meteoroid, having been spalled off by the shock wave at the instant it reached the rear surface. A typical fragment must have passed through the following stages during impact. First, it was heated and compressed by the shock wave. Its temperature at this point was equal to the sum of an 'adiabatic' and a 'residual' term and depended strictly on the shock intensity. A fraction of a millisecond later the rarefaction wave decompressed and cooled it to the residual temperature and threw it clear of the explosion area. From then on the fragment cooled by radiation and conduction. Its cooling time therefore depended on its size and ejection velocity and might be expected to range from a few seconds to a few minutes. If it chanced to fall on an area covered by hot ejecta, its cooling time would have been longer, up to several hours or days.

Few pressure indicators as such are available in iron meteorites. But because the reheating temperature is related to the shock intensity, it can serve as an indirect measure of the pressure to which the specimen was exposed. Two types of temperature indicators are available, differing in their response times. Diffusionless phase changes, such as melting or certain solid-state transformations, are prompt and can therefore record, in principle, the peak temperature reached during passage of the shock wave. Transition temperatures change with pressure, however, and this limits the usefulness of this class of temperature indicators.

Other structural changes involve diffusion of atoms from one phase into another and are therefore inherently slower. In one respect this is an advantage, because diffusion is negligible during the passage of the shock wave. The changes commence effectively only after decompression, when the specimen has cooled to the 'residual' temperature. Laboratory data at 1 atm are therefore strictly applicable. Inasmuch as the width of a diffusion zone depends on time as well as on temperature, it can serve as a measure of the cooling rate. A drawback of these indicators is their lack of specificity. They can also occur in an unshocked meteorite that happened to fall on a layer of hot ejecta. Fortunately, such cases are easily recognized by their abnormally slow cooling rates.

Temperature and Pressure Indicators

Several indicators exist, but they are very unevenly distributed over the range of interest. *Brentnall and Axon* [1962] have recently pub-

lished a detailed study of thermal alterations in Canyon Diablo, greatly extending our earlier work [*Lipschutz and Anders,* 1961*a*]. In the present discussion only those pressure and temperature effects that occur on a time scale of seconds, or faster, are of interest.

Changes in the metal. Two direct pressure indicators are available. Neumann lines (narrow lamellas in the kamacite, resulting from mechanical twinning along the 112 planes) require shocks of $\geq$80 kb at room temperature (P. S. De Carli, private communication, 1964), but they can also be produced by weaker shocks at lower temperatures. They seem to be present in most iron meteorites (Figure 1), having been produced during preterrestrial collisions or during impact with the earth. They are therefore of little use to us.

At pressures greater than 130 kb a transformation structure appears (Figures 2*a,* 2*b*), resulting from the temporary conversion of α- to ϵFe [*Smith,* 1958; *Maringer and Manning,* 1962]. In kamacite containing about 7% Ni, the transition pressure is probably lowered very slightly below 130 kb. The appearance of the ϵFe transformation structure changes with pressure. Smith noted that Armco iron subjected to shock pressures from 130 to 600 kb showed a progression of metallographic structures. 'Feathering' and multiplication of Neumann bands were followed at higher pressures first by a highly complex structure resembling carbon-free martensite and then by a simpler one. Analogous differences were found in meteoritic iron shocked to 190 and 600 kb (Figures 2*e,* 2*f*). At the lower pressure (Figure 2*e*) the Neumann bands begin to show a slight amount of feathering. The background is dense, fine-grained, and hard to resolve. At the higher pressure (Figure 2*f*) the Neumann bands show a well-developed transverse hatching, and the background has thinned out to a pattern of fine but sharp, clearly resolvable lines. In most Canyon Diablo meteorites studied the ϵFe structure resembled the 600-kb structure rather than the 190-kb structure.

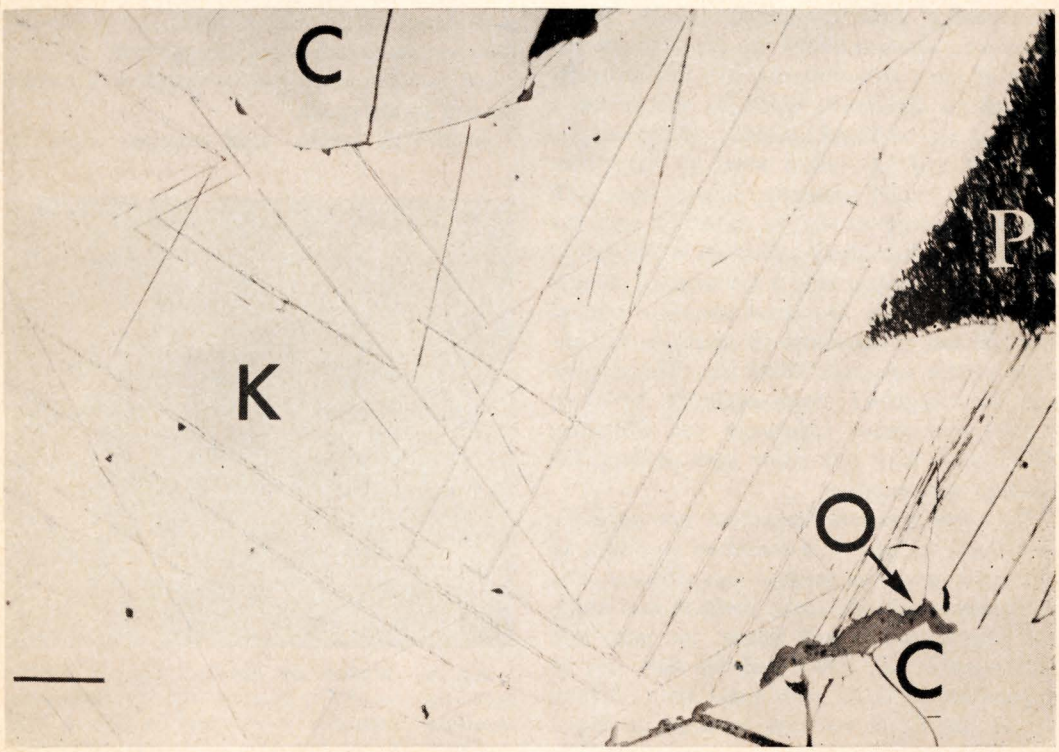

Fig. 1. Lightly shocked Canyon Diablo plains specimen (no. 1), rich in Neumann bands. C, cohenite; K, kamacite; O, iron oxide formed during terrestrial weathering; P, plessite. Scale bar, 100 μ.

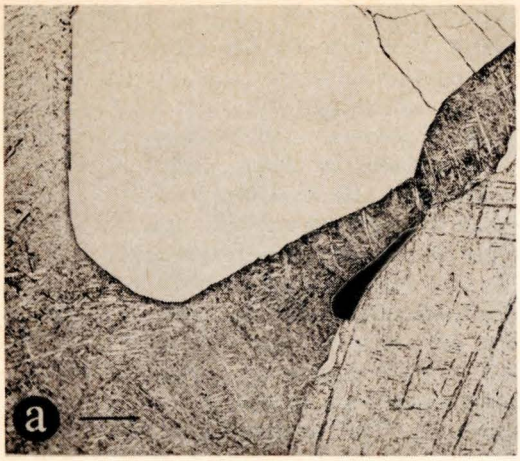

Fig. 2*a*. Moderately shocked Canyon Diablo specimen (no. 3), showing ϵFe transformation structure. Clear kamacite surrounding cohenite has transformed to dense, fine-grained structure. Vestiges of Neumann bands are visible in lower right. Compare with Figure 2*e*. Scale bar, 100 μ.

A disadvantage of this pressure indicator is its tendency to appear only in localized areas of favorable grain orientation [*Smith*, 1958]. Sample 3, which contains the low-pressure variety of the ϵ structure, displays this structure throughout the entire specimen, except for a patch of recrystallized kamacite. Other samples (e.g., 10 and 52) which seem to have been shocked to higher pressures, judging from both the morphology of the ϵ structure and the presence of other shock indicators in the 0.8- to 1-Mb range, contain only a few isolated patches of the ϵ structure. One must therefore scan at least 20 cm^2 of meteorite to ascertain the absence of this structure. Often the affected areas can be recognized macroscopically by their 'matte' appearance [*Maringer and Manning*, 1962]; they may etch either light or dark, depending on orientation.

No other pressure indicators are available from here on, and it is therefore necessary to infer pressures from residual temperatures. The relationship between shock pressure and residual temperature is well known for pure iron [*McQueen et al.*, 1962], and the data can be applied to kamacite with little error (Figure 3). In this figure we have assumed an initial temperature of +90°C, which seems to be the radiation temperature of iron meteorites at 1 AU [*Butler and Jenkins*, 1963].

Only a few subtle changes take place between the ϵFe transformation and 675°C, corresponding to a shock pressure of 970 kb. At about 500°C, a fine globular precipitate appears in the kamacite. *Brentnall and Axon* [1962] have called it 'microrhabdite' on the assumption that it consists of $(Fe, Ni)_3P$, but its exact nature has not been definitely established. It seems to form by some diffusionless transformation, for we have observed it in Odessa samples heated to 400°C for times as short as 15 seconds. Nearly all Canyon Diablo samples contain it, and since this structure can result from mere heating at low pressures (e.g., contact with hot ejecta) we cannot use it as an unambiguous pressure indicator.

At 550°C, a feathery precipitate of carbide appears at strain lines emanating from sharp corners of the cohenite [$(Fe, Ni)_3C$] crystals. At slightly higher temperatures, the cohenite begins to graphitize in cracks (Figure 4). A serious limitation of these two temperature indicators is their slowness. Both seem to require heating times of several minutes [*Brentnall and Axon*, 1962]. Hence they can hardly be used as shock indicators, though they may be quite useful in helping us to recognize sustained heating by hot ejecta.

At 675°C, carbon from cohenite begins to

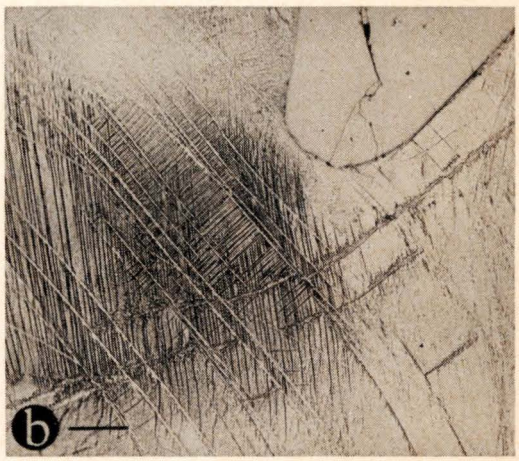

Fig. 2*b*. Moderately shocked Canyon Diablo specimen (no. 54C), showing ϵFe transformation structure. Kamacite background is clearer than in Figure 2*a*, but Neumann bands have developed sharp transverse hatching. This specimen matches the 600-kb, rather than the 200-kb, shock experiment (Figure 2*e*, 2*f*). Scale bar, 100 μ.

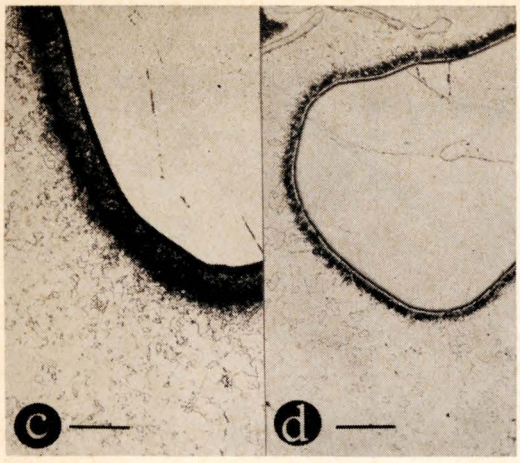

Fig. 2*c, d*. (*c*) Heavily shocked Canyon Diablo specimen (no. 55). Kamacite has recrystallized and carbon has diffused from cohenite into metal during excursion of kamacite into stability field of γFe. Owing to fast cooling rate, carbon diffusion zone transformed to martensite. Rows of fine blacks dots in cohenite consist of nodular graphite. Compare with Figure 2*g*. Scale bar, 100 μ. (*d*) Heavily shocked Canyon Diablo specimen (no. 33). Similar to 2*c*, but contains pearlite rather than martensite, owing to slower cooling rate. Scale bar, 100 μ.

diffuse into the surrounding kamacite, changing it to austenite (γFe saturated with carbon). The width of the diffusion zone depends on the reheating temperature and the time spent in the region above 675°C. The latter, of course, is a function of specimen size. On rapid cooling (less than a few minutes) the austenite changes to martensite, a metastable alloy of Fe and C. If the cooling time is slow, either because the meteorite was large or because it happened to be in contact with hot ejecta, the austenite decomposes to pearlite, a eutectoid of kamacite and cohenite (Figures 2*c*, 2*d*).

The carbon diffusion zone evidently forms *after* decompression of the meteorite, and the threshold temperature at 1 atm is therefore strictly applicable. Hence a meteorite displaying a carbon diffusion zone must have had a residual temperature of $\geq$675°C. Figure 3 shows that this implies a pressure of $\geq$970 kb.

At about 740°C and 1 atm, kamacite transforms to taenite (γFe). If Neumann bands or other imperfections are present in the kamacite, it becomes finely polycrystalline when the γ phase reverts to α phase on cooling (Figures

Fig. 2*e, f, g*. Samples of Odessa meteorite, shocked to 190, 600, and 1000 kb. Compare with Figures 2*a*–2*d*. Scale bar, 100 μ.

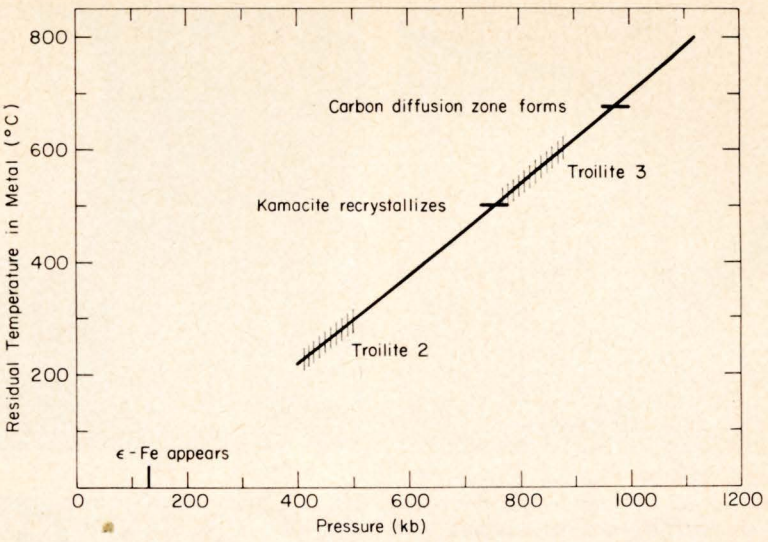

Fig. 3. Residual temperature in shocked iron, for an initial temperature of +90°C [*McQueen et al.*, 1962, and R. G. McQueen, private communication, 1965]. Metallographically observable changes in iron meteorites of about 7% Ni are also indicated. Vertical and horizontal markers indicate observed pressure and temperature thresholds, respectively. The thresholds for recrystallization of kamacite and melting of troilite are known only approximately.

2*c*, 2*d*). From Figure 3, a temperature of 740°C would imply a pressure of about 1 Mb. However, the γ-α transformation is diffusionless and can thus happen while the metal is still under pressure. At higher pressures, the transformation temperature drops. *Johnson et al.* [1962] have shown that shocked α Fe becomes polycrystalline whenever its temperature exceeds 775°K, the triple point of α-, γ-, and ϵFe. From Figure 3, this corresponds to a pressure of $\geq$750 kb.

However, Odessa meteorites artificially shocked to pressures of 400 to 500 kb show small amounts of recrystallized kamacite. Such localized recrystallization is invariably found only along fault lines or kamacite-taenite interfaces, regions where pressures may have been higher than in the body of the metal owing to multiple shock reflections.

Changes in troilite. Troilite can serve as a *P-T* indicator not only because the troilite itself undergoes several changes but also because troilite nodules are often associated with other minor phases [graphite, cohenite, and schreibersite, $(Fe,Ni)_3P$]. At temperatures between 900 and 1150°C, many characteristic binary and ternary eutectics form among these phases. Unfortunately, troilite nodules are relatively rare. Among the 45 uncut Canyon Diablo specimens in our initial suite, only 6 revealed troilite inclusions on cutting. No additional inclusions were detected by X-ray radiography, although 19 of the larger pieces were examined. To improve our statistics, five troilite-bearing Canyon Diablos (nos. 57–61) were obtained from Carleton Moore. Among the 11 specimens selected especially for their diamond content (nos. 46–56), 9 contained troilite, so that a total of 20 troilite-bearing specimens were available for our study.

Unfortunately, troilite cannot be used as a quantitative pressure indicator because its equation of state is not known. The generalizations discussed below are based largely on empirical correlations between changes in the troilite and metal.

The shock effects are always most prominent at the troilite-metal interface. In Odessa, the troilite at the interface is monocrystalline (see Figure 3*b* in *Lipschutz and Anders* [1961*a*]), but even in the lightly shocked Canyon Diablo specimens, showing nothing but Neumann bands, the troilite-pentlandite mixture at the periphery is polycrystalline, sometimes contain-

ing broken bits of Fe_3C and Fe_3P. The polycrystallinity is most easily observable in polarized light (Figures 5*a*, 5*b*). The grains are always finest at the periphery and coarsest in the interior of the nodule. The grain size seems to decrease with increasing shock pressure. Even though the grains are distorted and show deformation bands, they still retain their original orientation. In Table 1, we have designated such polycrystalline, but still oriented, troilite as '1' (Figures 5*a*, 5*b*).

In the more strongly shocked specimens, the troilite grains at the periphery no longer show their original orientation when viewed in polarized light. They are small, equiaxial, and randomly oriented. We have designated such equiaxial troilite as '2' in Table 1 (Figures 5*c*, 5*d*). It could have resulted from remelting or from a solid-state phase transformation during passage of the shock wave. Mere recrystallization by prolonged reheating is ruled out by both the resistance of troilite to recrystallization [*Curvello*, 1958] and the occasional localization of equiaxial grains along fault lines. The residual temperature cannot have been much above the melting point of troilite; otherwise, various binary and ternary eutectics would have formed from the schreibersite, cohenite, and kamacite surrounding the nodule.

Such eutectics are indeed present in the most strongly shocked specimens. The troilite at the periphery shows a distinctive polyphase structure, due to the presence of metal and other phases from the eutectic zone surrounding the nodule. We have regarded this polyphase structure as evidence for *remelting* and have designated such troilite as '3' in Table 1 (Figure 5*e*). In the interior of these nodules, the troilite is single-phase, consisting of large, randomly oriented, equiaxial grains (Figure 5*d*). These grains resemble troilite 2 in all respects except size and location and are therefore designated

Fig. 4. Lightly shocked Canyon Diablo specimen (no. 1), showing graphitization of cohenite in cracks. The cohenite (C) has broken down to graphite (black veinlets) and kamacite (light phase surrounding the graphite, corroded to grayish oxide in places). This graphitization may be the result of conductive heating by hot ejecta. Scale bar, 100 μ.

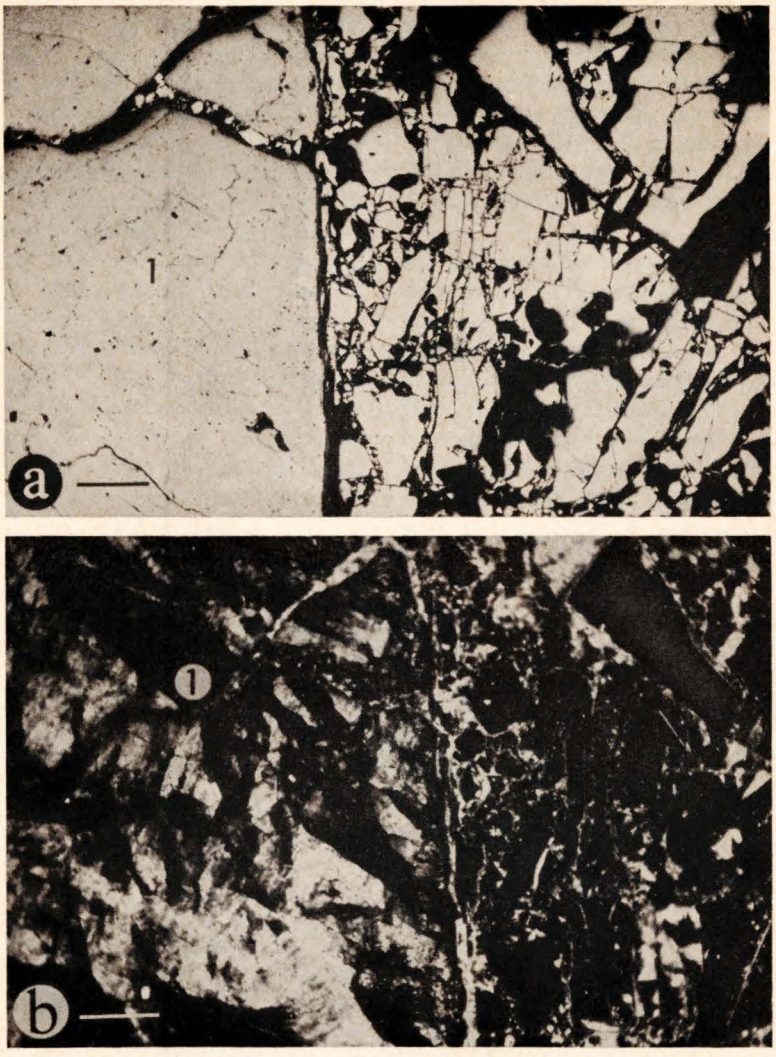

Fig. 5. Three stages of alteration of troilite, identified by numbers 1, 2, 3. Scale bar, 100 μ. (*a*) Troilite 1 in lightly shocked specimen (no. 12). The heavily fractured, light-colored material on the right is cohenite and schreibersite. Small, broken bits of both minerals are also found in the troilite near the interface. (*b*) Same field in polarized light. The originally monocrystalline troilite is seen to have broken down to a mixture of coarse but oriented grains. (*c*) Moderately shocked specimen (no. 54C) in polarized light. At the edge of the nodule (right), the troilite has changed to fine, unoriented, equiaxial grains ('troilite 2'). Further inward (left), the change has been less drastic; the grains are fine but still show their original orientation and are thus classified as troilite 1. (*d*) Coarser variety of troilite 2, in polarized light (specimen 30). (*e*) Remelted troilite 3, in specimen 52. Droplets show eutectic structure.


1
2
c

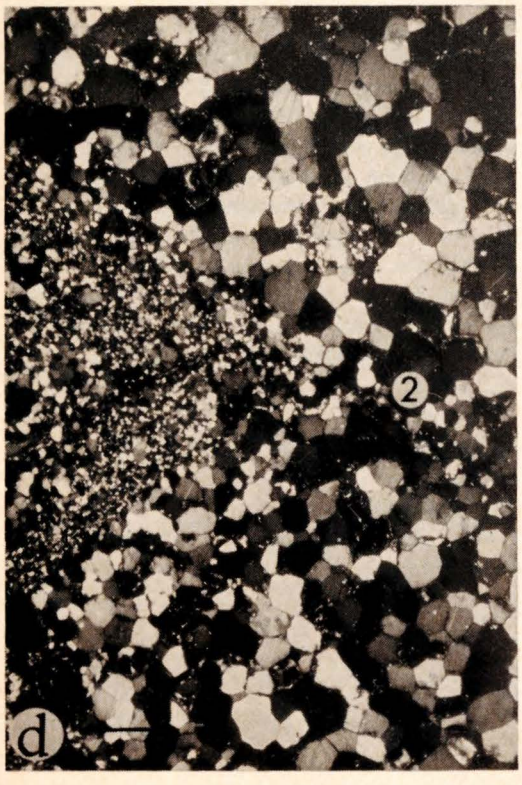
2
d

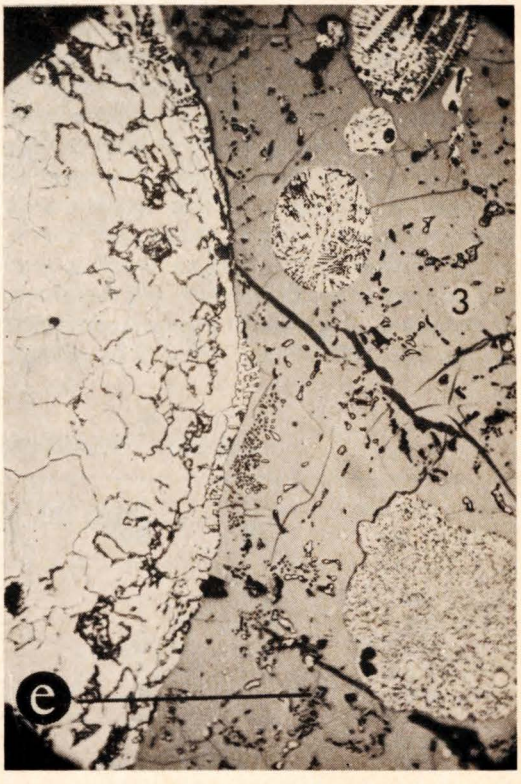
3
e

by the same symbol in Table 1. Shock experiments on Odessa gave troilite 2 at pressures as low as 400 to 500 kb; troilite 3 formed only at 700 to 800 kb. In Canyon Diablo, troilite 3 was correlated with extensively recrystallized kamacite, and troilites 1 and 2 were found also in samples showing only small amounts of recrystallized kamacite. This would seem to imply a pressure threshold near 700 kb for troilite 3, and ranges of about $\geq$130 to $\geq$1000 kb for troilite 2, and $<$130 to $<$800 kb for troilite 1.

Eutectics. Pure troilite has a melting point of 1193°C at 1 atm, but, in the presence of other meteoritic phases, various binary and ternary eutectics with melting points as low as 950°C form. The first signs of melting are usually found at the periphery of troilite nodules, where several minor phases exist in close contact. In addition to remelted troilite 3, strongly shocked meteorites usually contain phosphide eutectics (freezing points ~950 to 1000°C) and a carbide eutectic resembling ledeburite, the binary eutectic of Fe_3C and Fe. Pure ledeburite has a freezing point of 1147°C, but in the presence of troilite a ternary eutectic forms, with a freezing point of 1100°C. The effects of pressure are not known. We observed eutectics in an Odessa sample shocked to a nominal pressure of 700 to 800 kb, but in some of our Canyon Diablo samples eutectics were lacking even when the kamacite was completely recrystallized. Apparently, pressures somewhat greater than 800 kb are required to produce these eutectics. If the eutectics are used as pressure indicators, it must be kept in mind that they corrode more easily than the unmelted metal. The absence of eutectics thus does not preclude high pressures.

To provide some additional calibrations and cross checks of our pressure scale, we shocked 8 samples of the Odessa meteorite to pressures of 190 to 1000 kb. The shock effects observed are listed in Table 2. In a quantitative comparison of these data with Figure 3, it must be kept in mind that Figure 3 applies to pure iron initially at 90°C, whereas the samples in Table 2 contained 7% Ni and were initially at about 30°C. Also, the pressure gradients in the artificially shocked samples were very steep.

A summary of shock symptoms is given in Table 3. As noted in the table, some of these symptoms cannot, by themselves, be used to distinguish shock heating from conventional conductive reheating at low pressures (e.g., contact with hot ejecta). This ambiguity can usually be resolved if true pressure indicators (e.g., the ϵFe structure) are present or if the structure in question occurs in only one part of the specimen. Steep temperature gradients, as implied by such localization, could neither occur nor persist under conditions of prolonged, conductive reheating. A particularly telling piece of evidence is the presence of high-temperature regions in the interior. No conventional heat source can produce such 'inverse' temperature gradients [*Lipschutz and Anders,* 1961*a*].

TABLE 2. Shock Experiments on Odessa Meteorite*

Pressure, kb	Shock and Reheating Effects †					
	ϵFe	KRx	Cdiff	FeS	Eu	Diamonds‡
190	++					
200	++					
400–500	++	(+)		1, 2		+
500–600	++	(+)				
600	++	+				
700–800	+	+	p+	2, 3	L, Ph	+
1000		++	p++		L	
1000		++	p+	2, 3		+

* We are indebted to N. L. Coleburn of the Naval Ordnance Laboratory for the shock experiments at 190 and 600 kb and to P. S. DeCarli of the Stanford Research Institute for the remaining experiments.

† See Table 1 for explanation of symbols.

‡ So as not to destroy the textural relations, none of the presumed diamonds have as yet been removed for X-ray diffraction analysis. The identification must therefore be regarded as tentative.

TABLE 3. Shock Indicators in Canyon Diablo Meteorites

Symptom	Pressure, kb	Limitations*
Neumann bands	≤80 to ≈750	1
εFe transformation structure	≥130 to ≈750	2
Recrystallized kamacite	≥750	3*a*
Carbon diffusion zones	≥970	3*b*
Phosphide eutectics	>800	3*c*
'Ledeburite' eutectic	>800	3*d*
Troilite 1 (fine-grained, oriented)	<130 to <800	
Troilite 2 (equiaxial grains)	≥130 to ≥1000	
Troilite 3 (remelted)	≥750 ?	3*c*

* 1. May have been produced during breakup of meteorite parent body before it approached the earth.

2. Strong tendency toward localization.

3. Can also be produced by prolonged heating to (*a*) ≥500°C; (*b*) ≥675°C; (*c*) ≥950°C; (*d*) ≥1100°C; (*e*) a few hundred degrees. Such reheating can be ruled out if steep, 'inverse' temperature gradients are present or if characteristic symptoms of sustained reheating are absent.

Classification of Meteorites According to Shock Intensity

A serious obstacle to any classification scheme is the grossly nonuniform pressure distribution in shocked specimens. Often a given pressure indicator is found only in one part of the specimen, implying the existence of a pressure gradient across the meteorite. An example is shown in Figure 6, where a sharp boundary separates recrystallized kamacite from the εFe transformation structure. At higher pressures, a broad spectrum of pressure indicators is often found in a single specimen, especially in the presence of troilite. The diamond-bearing specimen 52 is a good example (Table 1; see also *Anders and Lipschutz* [1965]). Remelted troilite 3, ledeburite, and troilite 2 are found side by side with recrystallized and unrecrystallized kamacite, cohenite with and without martensite borders, etc. Very large pressure gradients evidently existed in some specimens.

In our classification scheme, we divided the meteorites into three categories. The dividing lines were chosen so as to make the assignments unequivocal in all cases. The classification was based entirely on the metal phase, since troilite inclusions were rarely present in our samples, and cohenite, though ubiquitous, was often highly localized.

1. *Heavily shocked* meteorites show completely recrystallized kamacite *throughout the entire sample*. Carbon diffusion zones around cohenite are present in at least a part of the specimen. These criteria imply a shock pressure of at least 750 kb in the entire sample and ≥970 kb in some portions.

2. *Lightly shocked* specimens show no shock symptoms other than Neumann bands, not even the εFe transformation structure. This implies pressures of ≤130 kb.

3. *Moderately shocked* specimens are the remaining ones. This category is somewhat heterogeneous, as implied by the widely spaced pressure limits (130–750 kb). To complicate matters further, some specimens show appreciable pressure gradients: carbon diffusion zones (≥970 kb) and phosphide or carbide eutectics (>800 kb) in some areas, unrecrystallized kamacite (≤750 kb) in others. To make our classification scheme as consistent as possible, we used the state of the kamacite as the overriding criterion. If unrecrystallized kamacite was present in only a part of the sample (implying that some regions did not reach pressures of as high as 750 kb), the meteorite was classified as moderately shocked, even though other portions showed evidence of shock pressures exceeding 1 Mb.

Four meteorites showed a peculiar kind of alteration: their cohenite was partly graphitized in cracks (see Table 1 and Figures 1*c* and 4). Such graphitization can be produced by reheating to about 650°C for times the order of an hour [*Brentnall and Axon*, 1962; *Lipschutz and Anders*, 1964]. Curiously, the Neumann bands, which were unusually abundant in all four specimens, had not recrystallized, although such recrystallization normally takes no more than a few hours at 650°C. This places rather narrow limits on the cooling times of these meteorites. To make matters worse, the cooling times of specimens in the 0.1- to 1-kg range are measured in minutes rather than hours, and it therefore seems likely that the cooling was retarded in some manner. Perhaps these meteorites were in contact with hot ejecta after the im-

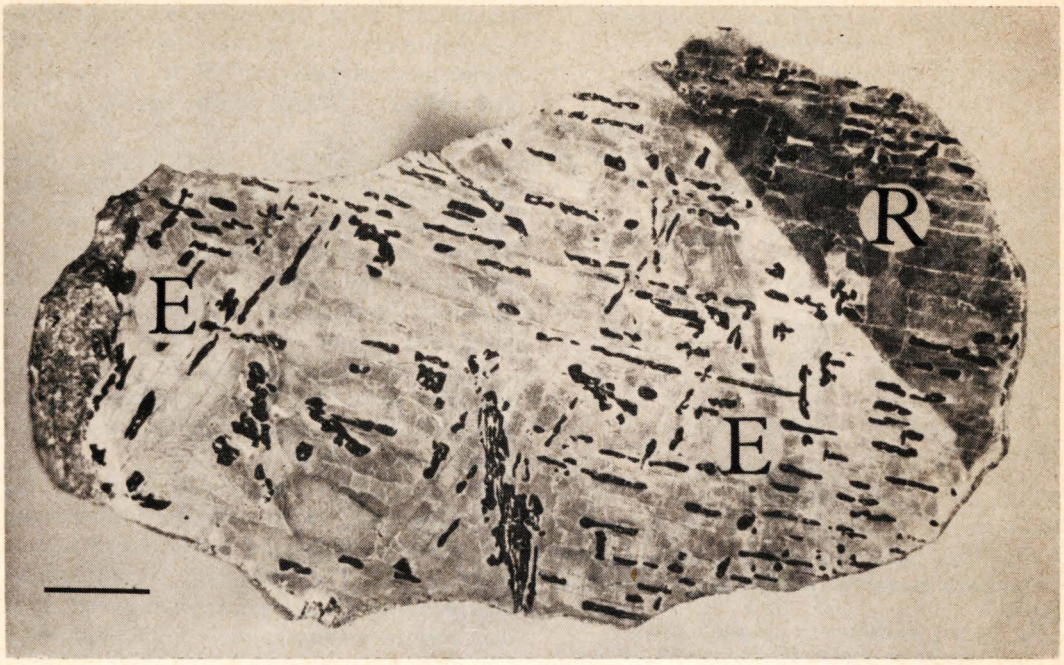

Fig. 6. Pressure gradients in specimen 3. In the main part of the specimen, the kamacite contains the ϵ structure (E). In the darker part at the upper right, no ϵ structure is present; the kamacite is completely recrystallized (R). In the wedge-shaped, light-colored zone at the lower right, between letters 'E' and 'R,' both the ϵ structure and recrystallized kamacite are present. Scale bar, 1 cm.

pact. There was no apparent regularity in the distribution of these meteorites. They were located west, south, and east of the crater. None of the other meteorites in the same section showed signs of such prolonged reheating, and we therefore suspect that the alteration was caused either by large blocks of hot rock or by a highly localized, ray-like blanket of hot 'rock flour' or impactite. Consequently, these effects were disregarded in the classification of the specimens.

Mass Spectrometry

To measure the stable isotopes of He, Ne, and Ar, we evaporated a meteorite sample from a hot crucible, purified the released gases, and put the remaining gas into a Nuclide Analysis Associates RSS-1, 4.5-inch-radius mass spectrometer. The sensitivity of the instrument was calibrated with known amounts of He^3, He^4, Ne, and Ar. Instead of performing a separate calibration before and after the measurement of a sample, we added the calibration standards to the sample gas in most cases and measured the resulting increments of signals. The ion source of the mass spectrometer was operated without a source magnet; emission currents ranged from 0.03 to 0.6 ma, depending on the ion beam intensity. With an extraction potential of 1800 volts, the focusing conditions were almost identical at all masses concerned, so that a given set of focusing conditions could be used throughout an entire run. Whenever a change in ion beam intensity of more than 2% occurred during a measurement, the focusing conditions were checked and the measurement repeated.

The ion current was deflected on the first dynode of a nine-stage secondary electron multiplier with a gain of about 10^4 at an over-all electron accelerating voltage of 1.5 kv. The signal produced by the current across a 10^{10}-ohm resistor was amplified by a vibrating reed electrometer and recorded. All peaks were measured by magnetic scanning, each peak being scanned several times. In addition to the peaks resulting from the rare gas isotopes, a number of peaks at other masses were measured as controls. This

included peaks at masses 1, 2, 16, 18, 28, 35, 37, and 44. A typical sensitivity for He^3 under the conditions given (emission current 0.3 ma, ion accelerating voltage 1800 volts, multiplier gain 10^4, resistor 10^{10} ohms) was 60–100 mv for 10^{-8} cc STP of gas. The mass spectrometer could be outgassed at 350°C.

It was expected that the study of a large number of specimens of the massive Canyon Diablo iron meteorite would present some difficulties, inasmuch as the cosmogenic rare gas content might vary appreciably. Indeed, the He^3 values ranged from ≤ 0.03 to 294×10^{-8} cc STP/g. As far as He^3 is concerned, the mass spectrometer always has a background peak at mass 3 resulting from H_3^+ ion molecules. Since the concentration of this species depends on the partial pressure of hydrogen, it was important to purify the gas as thoroughly as possible, particularly for specimens with low He^3 contents.

Initially the gas was purified by means of a titanium metal getter enclosed in a thick-walled stainless steel cylinder connected to the vacuum line by a glass-to-metal seal. The titanium was heated to about 900°C for 20 to 30 minutes by means of a resistance-heated furnace and then allowed to cool to room temperature. This procedure yields satisfactory backgrounds at mass 3, but takes much time. Equally low backgrounds were attained by another and faster technique. The meteorite samples were dropped into a prebaked alumina crucible (Figure 7) which was then heated to about 1750°C by induction heating with an external load coil. This arrangement allows the gas to be purified at the same time. A second molybdenum crucible was mounted below the 'melting' crucible and filled with titanium metal sponge. Two 6-mm holes were drilled through the wall of the lower crucible to permit unimpeded diffusion of gas to the getter. The lower crucible was positioned at the fringe of the RF field; its temperature during the melting of a sample was therefore somewhat lower than the temperature of the upper crucible but high enough for the gettering of N_2, O_2, and the like. Most samples were heated to about 1750°C for 20 minutes, which was long enough to evaporate Ni-Fe specimens weighing 0.1 to 2.0 grams. Hydrogen is efficiently adsorbed only at temperatures below 500°C; hence the H_2 gettering took place while the furnace cooled to room temperature. It was found that this cooling took about 45 minutes.

In a few instances it was observed that the melting or evaporation of a sample had not been complete, and in such cases all data were discarded. In separate runs of specimens 20 and 38 the temperature was increased stepwise in 100°C increments starting at 900°C. (Temperatures were measured with an optical pyrometer and are probably accurate to within 20°C.) It was found that only about 10% of the cosmogenic He^3 was released up to the melting point of the metal, but the amount rose to

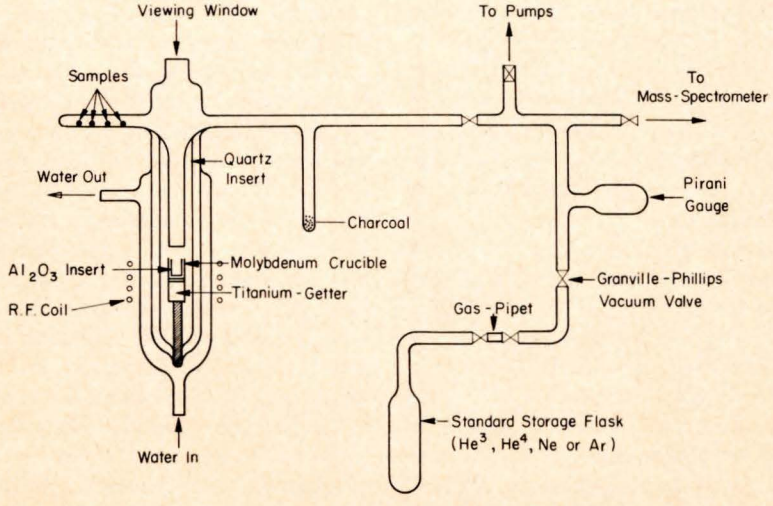

Fig. 7. Schematic drawing of the furnace and the calibration system. The volume of the gas pipet is 0.1 cc.

more than 95% by the time the sample had completely melted.

Backgrounds at masses 3 and 4 were determined in blank runs, which were alternated periodically with sample runs. A typical background at mass 3 was equivalent to 10^{-10} cc STP of He^3. A typical He^4 background was 5×10^{-8} cc STP, but this value depended somewhat upon the timing because He^4 from room air diffused through the Pyrex walls of the system. We compared He^4 blanks obtained from a water-cooled Pyrex furnace with backgrounds obtained from an identical furnace made from Corning 1720 combustion tubing and found no significant differences for blank runs between the two glasses.

Another problem was the possibility of contamination of the mass spectrometer (or contamination from the gas inlet system and furnace), particularly when a sample with high gas content was followed by a sample with low gas content. All samples with more than 1×10^{-8} cc STP/g of He^3 were always remelted and the released gas measured. In spite of this precaution it was observed in some instances that contamination from He^3 existed that could interfere with the next sample. Because of this fact and its implications for the measurements of Ne and Ar, a preliminary survey of all specimens was made first in which only He^3 was measured. For this survey the specimens were chosen at random. Several times the measured He^3 content of consecutive samples measured in a clean furnace was low. Such specimens were measured only once and are marked in Table 1. The precision of these values is perhaps smaller than the precision of duplicate measurements, but this fact is of minor consequence in the present study. Taking a conservative view, we can assume that these single measurements are valid to within a factor of 2.

According to the results of this survey the meteorites were divided into three groups. The first group had $He^3 > 10 \times 10^{-8}$ cc STP/g. For a number of meteorites in this group all the stable isotopes of He, Ne, and Ar were measured. The second group consisted of specimens with He^3 between 1 and 10×10^{-8} cc STP/g. For this group the He^3 background was not yet serious and amounted to 15% at most. He^4, Ne^{21}, and Ar^{38} values in this group are not reliable because of background interference and are not reported. The third group consisted of specimens with $He^3 < 1 \times 10^{-8}$ cc STP/g. Sometimes the signal at mass 3 could not be distinguished from the variations in backgrounds from blank to blank. In such cases it was assumed that the signal at mass 3 represented an *upper limit* to the He^3 content of the specimen. The results of such runs are accordingly given as upper limits of the He^3 content.

The measurement of He^4, Ne, and Ar isotopes presented no special problems. As usual, Ar was first adsorbed on charcoal while He and Ne were measured. After the completion of the He-Ne measurement the spectrometer was evacuated before Ar was released from the trap. There were, of course, background corrections for Ne^{21}, Ar^{36}, and Ar^{38}. The amount of the correction depended mainly on the degree of outgassing of the furnace. Each furnace was prebaked to 1750°C for 6 to 8 hours whenever it had been exposed to the atmosphere. Typical backgrounds were: Ne^{20}, 1×10^{-8} cc STP; Ar^{40}, 10×10^{-8} cc STP.

He^3 and He^4 results were corrected for background with the average He^3 and He^4 values of the preceding and following blanks. For the correction of Ne^{21} it was assumed that the neon was a mixture of cosmogenic gas with $Ne^{20} : Ne^{21} : Ne^{22} = 1 : 1 : 1$ and air neon. It was assumed that all of the observed Ar^{40} was air contamination. Whenever the background correction of He^4, Ne^{21}, or Ar^{38} exceeded 30%, the result was discarded.

For the calibration of the mass-spectrometer sensitivity, metered amounts of He^3, He^4, Ne, and Ar were added to the sample gases from storage bulbs by means of all-metal gas pipets and the increments of signals at given masses were measured. Since the ratio of bulb volume to pipet volume was large, the calibrations did not affect the standard gas in the reservoirs. The pipets, being of a new design, were carefully checked. It was found that the measurement of ten successive standards was reproducible to within 0.5%. This test was repeated several times and no change in reproducibility was found. Although this did not mean that the volume of the pipet had remained unchanged, there was independent evidence from repeated measurements of the same specimen that the volume remained constant to within at least 2.5% and probably much less.

TABLE 4. Cosmogenic He, Ne, and Ar in Canyon Diablo Irons

Sample	Cosmogenic Rare Gases, 10^{-8} cc STP/g					Ratios				Radiation Age, m. y.
	He^3	He^4	Ne^{21}	Ar^{36}	Ar^{38}	He^3/He^4	He^3/Ne^{21}	He^3/Ar^{38}	Ar^{38}/Ar^{36}	
24	294	1046	3.80	11.8	17.7	0.281	77	16.6	1.50	980
13	174	637	2.22	7.19	11.2	0.273	78	15.5	1.56	622
38	109	435	1.27	4.93	7.16	0.251	86	15.2	1.45	551
7	109	427	1.26	4.17	6.46	0.250	87	16.9	1.55	538
20	65.5	278	0.67	2.56	3.87	0.236	98	16.9	1.51	578
23	46.8	191	0.47	1.86	2.86	0.245	100	16.4	1.54	470
43a*	40.2	151	0.47	1.60	2.35	0.266	86	17.1	1.47	181
26	36.2	151	0.35	1.40	2.20	0.240	103	16.5	1.57	468
47	35.2	154	0.33	1.42	2.10	0.229	107	16.8	1.48	553
43b*	33.6	131	0.38	1.29	1.99	0.256	88	16.9	1.54	166
54A	33.1	150	0.32	1.44	2.2	0.221	103	15.0	1.53	468
11	21.9	93.3	0.25	0.94	1.46	0.235	88	15.0	1.55	122
44	14.7	66	0.14	0.53	0.82	0.223	105	17.9	1.55	191
27	12.2	55	0.11	0.51	0.82	0.223	110	14.9	1.61	248
II†	36.8	151	0.34	1.3	2.3	0.240	108	16.0	1.77	640
III†	175	664	1.92	6.53	10.3	0.264	92	17.0	1.58	1030

* Samples 43a and b were taken from different portions of specimen 43. In all other cases, adjacent samples of the same slice were used for duplicate measurements.

† These were the anomalous Canyon Diablo 2 and 3 meteorites previously described by *Heymann* [1964]. Their original specimen numbers were 371.2 and 586.1.

The results of the He^3 measurements are shown in Table 1. We estimate the precision as 5% for specimens with $He^3 > 10 \times 10^{-8}$ cc STP/g and as 5–10% for the specimens with He^3 between 1 and 10×10^{-8} cc STP/g. We believe that any He^3 value smaller than 10^{-8} cc STP/g is correct to within at least a factor of 2.

The He^3, He^4, Ne^{21}, and Ar^{38} data are given in Table 4. The errors of He^4, Ne^{21}, and Ar^{38} are estimated to be 5% whenever the He^3 content is more than 30×10^{-8} cc STP/g and somewhat larger, probably 7 to 10%, for the remaining specimens.

3. Results and Discussion

Cosmic Ray Exposure Age

One of the objectives of this study was the determination of the cosmic ray exposure age of Canyon Diablo. The noble-gas content of a given meteorite sample is a function of both its preatmospheric depth and its exposure age. Some information on the depth is usually needed before an age can be calculated. However, *Signer and Nier* [1960] have developed an ingenious method for determining both the age and depth from noble-gas data alone. Their method is based on the principle that the production cross sections of various cosmogenic nuclides in iron meteorites differ in their energy dependence. Some nuclides, such as Ne^{21}, are made mainly by high-energy primaries; others, such as He^3, are also made in appreciable yield by low-energy secondaries. Consequently, the He^3/Ne^{21} ratio increases with depth and can serve as a depth indicator. Signer and Nier have determined, for meteorites of various masses, the relationships between depth-sensitive ratios (e.g., He^3/Ne^{21}) and the production rates of cosmogenic nuclides (e.g., atoms Ar^{38} g^{-1} yr^{-1}). On a plot of He^3/Ne^{21} versus Ar^{38} all samples of a single meteorite having the same age lie on a single curve while samples of higher or lower age are displaced to the right or left.

When the data for the 14 Canyon Diablo samples with the highest gas contents are plotted on such a graph, they fall into two, or possibly three, distinct groups (Figure 8). Each group of points follows remarkably closely Signer and Nier's curve for a meteoroid of 'infinite' mass (i.e., $\gg 2 \times 10^8$ g). The position of the first two curves corresponds to ages of 170 and 540 m.y., assuming an age of 640 m.y. for the 'reference'

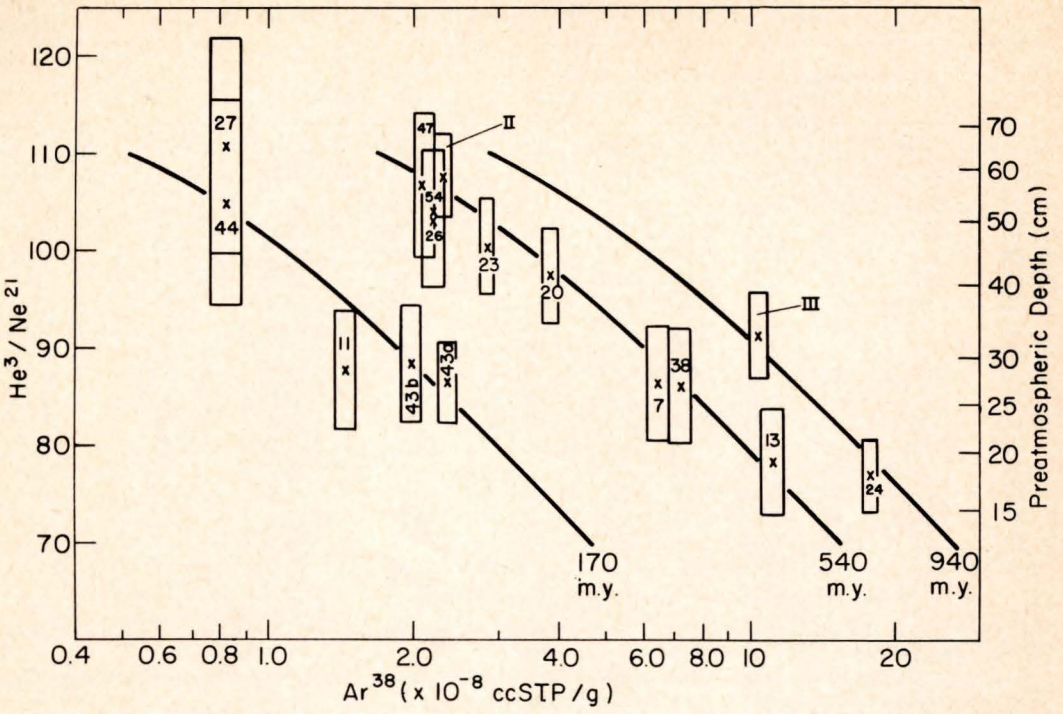

Fig. 8. He^3/Ne^{21} ratio versus Ar^{38} content for 14 Canyon Diablo meteorites. Points II and III are previously published measurements on the anomalous Canyon Diablo 2 and 3 [*Heymann,* 1964]. Solid lines are isochrons of *Signer and Nier* [1960], constructed from data supplied by P. Signer.

meteorite Grant [*Signer and Nier,* 1960; *Schaeffer and Heymann,* 1965; *Voshage and Hess,* 1964; *Lipschutz et al.,* 1965].

The two remaining points appear to fit a 940-m.y. curve. Alternatively, these two samples might have come from a projection of the main mass which was less heavily shielded than the remainder [*Heymann,* 1964]. The exposure age of sample 24, as measured by the K^{41}/K^{40} method, is only 620 ± 130 m.y. (J. Okano and H. Voshage, private communication). This would seem to support the latter alternative. Sample 13, on the other hand, has a K^{41}/K^{40} age of 565 ± 120 m.y., which agrees rather well with our figure of 540 m.y.

It is not surprising that Canyon Diablo shows two different ages. This has also been observed for several other large iron meteorites: Sikhote-Alin [*Vilcsek and Wänke,* 1961], Odessa [*Vilcsek and Wänke,* 1963], and Arispe [*Lipschutz et al.,* 1965]. These meteorites apparently suffered secondary collisions some time after the primary collision that shattered their parent bodies. These secondary collisions created new surfaces, thereby exposing previously shielded material to cosmic-ray bombardment. The lesser ages correspond to the dates of these secondary collisions (provided that the newly exposed material had no previous irradiation history).

Figure 9 shows the geographic distribution of the two age groups. No clear-cut, systematic trends are evident. A somewhat intriguing fact is that the meteorites with 170-m.y. ages are concentrated in a 120° sector south of the crater. Was the 'new' surface facing south as the meteorite struck the ground? Perhaps so, but in view of the limited statistics no definite conclusions can be drawn.

During this study we also measured the noble-gas contents of the atypical Canyon Diablo 2 and 3 meteorites. Both are medium octahedrites, whereas 'normal' Canyon Diablo 1 is a coarse octahedrite [*Nininger,* 1940, 1956; *Nininger and Nininger,* 1950]. The Ni content of Canyon Diablo 2, 8.22%, is also distinctly higher than that of Canyon Diablo 1, 7.11% [*Goldberg et*

al., 1951]. The noble-gas data, which have been published elsewhere [*Heymann*, 1964], indicate that Canyon Diablo 2 and 3 were neither distinct falls nor satellites of the main mass but were located *inside* the main mass at the time of fall. This result provides some quantitaive information on the compositional uniformity of meteoritic iron. The (equivalent spherical) diameter of the Canyon Diablo object seems to have been of the order of 25 or 86 m, depending on the mass estimate: 6.3×10^{10} grams [*Shoemaker*, 1960] or 2.6×10^{12} grams [*Öpik*, 1958]. *Öpik* [1961] has recently presented new, compelling arguments supporting his earlier estimate. Whichever value is accepted, it is clear that major compositional and structural differences existed in meteoritic iron over distances of less than 100 m. This is not surprising; *Lovering* [1957] has pointed out that slow freezing of a Ni-Fe melt will give crystals varying continuously in Ni content. His attempt to account for all iron meteorites by differentiation of a single melt has been criticized [*Anders*, 1964], but there is no doubt that some differentiation processes of this type must have occurred during the formation of the iron meteorites.

Shock Effects, Location, and Preatmospheric Depth

The He^3 measurements for all 56 specimens are shown in Figure 10. An approximate depth scale is also shown, based on a half-thickness of 15 cm for the production of He^3 and an exposure age of 540 m.y. Unfortunately, the existence of a second age group at 170 m.y. makes the correlation between He^3 and depth somewhat ambiguous for the 44 samples whose ages were not determined. It was not feasible to measure Ne^{21}, Ar^{38}, and He^4 in most of these samples, since atmospheric contamination becomes a serious problem at these mass numbers long before it begins to interfere with the measurement of He^3.

To reduce all data to a common basis insofar as possible, we raised the measured He^3 contents of the 5 samples with an age of 170 m.y. by a factor of $540/170 = 3.18$ and plotted the corrected values in Figure 10. For the remaining 44 samples no correction could be applied. Judg-

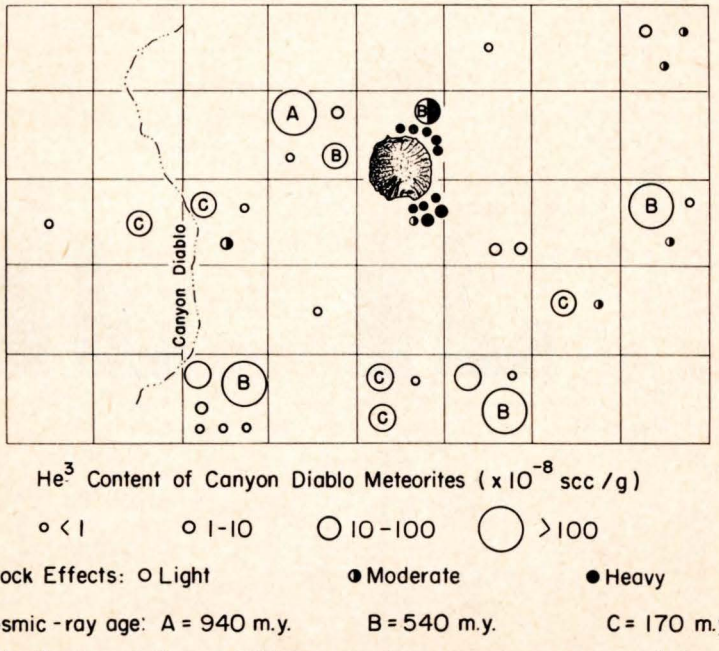

Fig. 9. Distribution of Canyon Diablo meteorite samples 1 to 45 around the crater. Section numbers marked in corners of 1-mile squares correspond to those in Table 1. One rim specimen (no. 47) and a specimen from an unknown location (no. 54A) also have cosmic-ray ages of 540 m.y.

ing from the results on the 14 dated samples, perhaps one-half of the 44 undated ones might have ages of 170 m.y. This would require an increase of their He^3 contents by a factor of 3.18 and a decrease of their depth by 25 cm.

A remarkable fact is the relatively shallow origin of most samples. All but 10 of the samples definitely come from a depth of less than 1.8 m. For these 10, only an upper limit for the He^3 content was determined. Even if we make the (probably unwarranted) assumption that these samples came from the interior of the meteoroid, it is remarkable that so few such 'interior' samples were found. For an original mass of 2.6×10^{12} grams, only 12% of the total mass is contained in the outermost 1.8 m, but even for Shoemaker's estimate of 6.3×10^{10} grams it would be only 38%. But 82% of our samples come from this 1.8-m layer. For the rim specimens alone, the percentage is 78%. (Most of our samples were of nearly equal weight, so that this conclusion would not be changed appreciably if the calculation were done on the basis of weight rather than number.) Our findings therefore support *Öpik's* [1958] conclusion that the surviving Canyon Diablo fragments came from the rear surface of the projectile.

If we examine the histograms in Figure 10 in detail, we observe some rather marked correlations.

Shock and location. Seventy-two per cent of the rim specimens, but none of the plains specimens, are classified as heavily shocked. (Whenever possible, the figures quoted in this section also include specimens 57 to 61, for which only metallographic data were available.) If the moderately shocked specimens are included, we see that 100% of the rim specimens, but only 14% of the plains specimens, have been shocked to $\geq$130 kb. These results certainly bear out *Nininger's* [1956] earlier observations, although he seems to have overlooked the existence of a few shocked plains specimens. This is understandable because the effects of moderate shock, resulting in reheating to less than 675°C, are subtle and hard to recognize.

It is rather remarkable that 4 of the 5 moderately shocked plains specimens are located northeast and southeast of the crater—the same directions where most of the rim specimens are found. It seems that the throwout pattern for the deeper, strongly shocked layers of the meteorite was highly directional. The metallic spherules collected by *Nininger* [1956] show

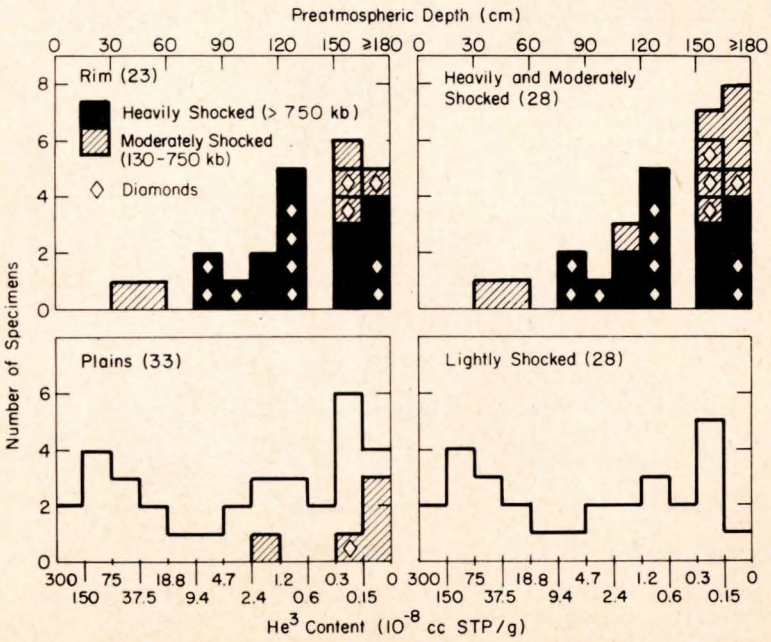

Fig. 10. Correlation of shock effects with location and depth.

TABLE 5. Correlations between Shock Effects and Depth for Various Categories

Category	Number	Mean Depth, cm	Shock Effects		
			Light, %	Moderate, %	Heavy, %
Plains	36	81	86	14	0
Rim (all)	25	127	0	28	72
Rim (with diamonds)	14	133	0	29	71
Rim (without diamonds)	11	121	0	27	73
Lightly shocked	31	72	100	0	0
Moderately to heavily shocked	30	132	0	40	60
Diamond-bearing	15	135	0	33	67

the same northeast-southeast concentration pattern, indicating that the directionality persisted through the stage during which the meteorite was vaporized.

Location and depth. The rim and plains populations also differ in mean preatmospheric depth. Both distributions contain a similar number of interior samples, but they differ markedly in the proportion of near-surface samples. The rim specimens come from a mean depth of 121 cm and the plains specimens come from 81 cm. No systematic differences are found within the plains population itself. Specimens located 1 to 4 km from the center of the crater come from the same mean depth as those located at distances greater than 4 km. These mean depths are geometric means. Systematic age differences can account for only part of this difference. If the extreme assumption is made that the age of all rim specimens is 170 m.y. and all plains specimens 540 m.y., the mean depths become 96 and 81 cm. But if such a trend exists, it is certainly in the wrong direction. Only three rim specimens have been dated, but the age of all three is 540 m.y.

The two histograms in the right-hand part of Figure 10 suggest a further correlation between shock heating and depth. One might at first suspect that this correlation is a spurious one, the low He^3 contents merely reflecting extensive gas losses in reheated specimens, but this seems most unlikely. The shock itself could hardly have driven out any He^3 in the available times of less than 10^{-3} sec. After decompression, the samples cooled from some initial temperature in the range 700–1000°C to no more than a few hundred degrees in a few minutes. As mentioned earlier, the cooling time was as long as several hours in a few cases, probably because the samples were in contact with hot ejecta. But one of these samples (no. 24) happens to have the highest He^3 content observed in this study. In agreement with this finding, diffusion data show that expulsion of 10% of the cosmogenic He^3 in iron meteorites requires 24 hours at 900°C and 2400 hours at 760°C [*Fechtig et al.*, 1963]. Hence it is most unlikely that the observed distribution is seriously affected by He^3 losses during cooling.

To some extent, the shock-depth correlation merely reflects the location-depth correlation, since most shock-heated specimens come from the rim. But there are two other lines of evidence strengthening this correlation. The five reheated plains specimens come from depths of more than 1 to 1.5 m, and the heavily shocked specimens come from a greater mean depth than the moderately shocked ones: 136 versus 114 cm.

The data on the 15 diamond-bearing samples are of interest. At least 13 and probably 14 of these come from the rim and are either moderately or heavily shocked. The fifteenth (no. 5) is a plains specimen, but it, too, shows evidence of shock in the range 130–750 kb. This correlation would seem to support the view that the diamonds were produced by impact [*Nininger*, 1956; *Lipschutz and Anders*, 1961*a*, *b*; *Anders and Lipschutz*, 1965]. An interesting question is whether the diamond-bearing specimens form a distinct subgroup among the rim specimens [*Carter and Kennedy*, 1964]. Our data do not support this view. Diamond-bearing and diamond-free rim specimens cover about the

same depth range and include about the same proportion of moderately and heavily shocked specimens (Table 5).

Acknowledgments. We thank Dr. O. A. Schaeffer, Brookhaven National Laboratory, for his kind assistance in preparing the gas standards and for supplying a furnace of Corning 1720 combustion glass.

This work was supported in part by the National Aeronautics and Space Administration grant NsG-366 and the U. S. Atomic Energy Commission contract AT(11-1)-382. E. Anders is indebted to the National Science Foundation for a Senior Postdoctoral Fellowship and to the University of Berne for a Visiting Professorship. M. E. Lipschutz gratefully acknowledges the National Science Foundation for a Postdoctoral Fellowship at the University of Berne.

References

Anders, E., Origin, age, and composition of meteorites, *Space Sci. Rev., 3,* 583–714, 1964.

Anders, E., and M. E. Lipschutz, Critique of paper by N. L. Carter and G. C. Kennedy, 'Origin of diamonds in the Canyon Diablo and Novo Urei meteorites,' *J. Geophys. Res., 71,* 643–661, 1966.

Arnold, J. R., M. Honda, and D. Lal, Record of cosmic-ray intensity in the meteorites, *J. Geophys. Res., 66,* 3519–3533, 1961.

Barringer, D. M., Meteor Crater (formerly called Coon Mountain or Coon Butte) in northern central Arizona. Read before the National Academy of Sciences at its Autumn Meeting at Princeton University, November 16, 1909 (privately published).

Brentnall, W. D., and H. J. Axon, The Response of Canyon Diablo meteorite to heat treatment, *J. Iron Steel Inst., London, 200,* 947–955, 1962.

Butler, C. P., and R. J. Jenkins, Temperature of an iron meteoroid in space, *Science, 142,* 1567–1568, 1963.

Carter, N. L., and G. C. Kennedy, Origin of diamonds in the Canyon Diablo and Novo Urei meteorites, *J. Geophys. Res., 69,* 2403–2421, 1964.

Curvello, W. da Silva, Meteoritic sulphides, *Bol. Museu Nacl. (Rio de Janeiro), Geol., 27,* 1–44, 1958.

Fechtig, H., W. Gentner, and P. Lämmerzahl, Argonbestimmungen an Kaliummineralien, 12, Edelgasdiffusionsmessungen an Stein- und Eisenmeteoriten, *Geochim. Cosmochim. Acta, 27,* 1149–1169, 1963.

Goldberg, E., A. Uchiyama, and H. Brown, The distribution of Ni, Co, Ga, Pd, and Au in iron meteorites, *Geochim. Cosmochim. Acta, 2,* 1–25, 1951.

Heymann, D., Origin of the Canyon Diablo No. 2 and No. 3 meteorites, *Nature, 204,* 819–821, 1964.

Johnson, P. C., B. A. Stein, and R. S. Davis, Temperature dependence of shock-induced phase transformations in iron, *J. Appl. Phys., 33,* 557–561, 1962.

Ksanda, C. J., and E. P. Henderson, Identification of diamond in the Canyon Diablo iron, *Am. Mineralogist, 24,* 677–680, 1939.

Lipschutz, M. E., and E. Anders, The record in the meteorites, 4, Origin of diamonds in iron meteorites, *Geochim. Cosmochim. Acta, 24,* 83–105, 1961*a*.

Lipschutz, M. E., and E. Anders, On the mechanism of diamond formation, *Science, 134,* 2095–2099, 1961*b*.

Lipschutz, M. E., and E. Anders, Cohenite as a pressure indicator in iron meteorites? *Geochim. Cosmochim. Acta, 28,* 699–711, 1964.

Lipschutz, M. E., P. Signer, and E. Anders, Cosmic ray exposure ages of iron meteorites by the Ne^{21}/Al^{26} method, *J. Geophys. Res., 70,* 1473–1489, 1965.

Lovering, J. F., Differentiation in the iron-nickel core of a parent meteorite body, *Geochim. Cosmochim. Acta, 12,* 238–252, 1957.

Maringer, R. E., and G. K. Manning, Some observations on deformation and thermal alterations in meteoritic iron, in *Researches on Meteorites,* edited by C. B. Moore, pp. 123–144, John Wiley & Sons, New York, 1962.

McQueen, R. G., E. Zukas, and S. Marsh, Residual temperatures of shock-loaded iron, paper presented at American Society for Testing Materials Symposium on Dynamic Behavior of Materials, *ASTM Spec. Publ. 336,* 1962.

Nininger, H. H., Diamonds in Canyon Diablo, Arizona, meteorites, *Popular Astron., 47,* 504–507, 1939.

Nininger, H. H., A new type of nickel-iron meteorite from the vicinity of the Arizona meteorite crater, *Popular Astron., 48,* 328–332, 1940.

Nininger, H. H., Structure and composition of Canyon Diablo meteorites as related to zonal distribution of fragments, *Popular Astron., 58,* 169–173, 1950.

Nininger, H. H., *Arizona's Meteorite Crater,* American Meteorite Museum, Sedona, Arizona, 1956.

Nininger, H. H., and A. D. Nininger, *The Nininger Collection of Meteorites,* American Meteorite Museum, Winslow, Arizona, 1950.

Öpik, E. J., Meteorite impact on solid surface, *Irish Astron. J., 5,* 14–33, 1958.

Öpik, E. J., Notes on the theory of impact craters, *Proc. Geophys. Lab.–Lawrence Radiation Lab. Cratering Symp.,* Washington, D. C., March 28–29, 1961, *2,* Paper S, 1–28, *Lawrence Radiation Lab. Rept. UCRL-6438,* 1961.

Schaeffer, O. A., and D. Heymann, Comparison of Cl^{36}-Ar^{36} and Ar^{39}-Ar^{38} cosmic ray exposure ages of dated fall iron meteorites, *J. Geophys. Res., 70,* 215–224, 1965.

Shoemaker, E. M., Penetration mechanics of high velocity meteorites, illustrated by Meteor Crater, Arizona, *Intern. Geol. Congr., 21st, Copenhagen, 1960, Rept. Session, Norden 18, Struc-*

ture of the Earth's Crust and Deformation of Rocks, Copenhagen, 1960.

Signer, P., and A. O. Nier, The distribution of cosmic-ray-produced rare gases in iron meteorites, *J. Geophys. Res., 65,* 2947–2964, 1960.

Smith, C. S., Metallographic study of metals after explosive shock, *Trans. AIME, 212,* 574–589, 1958.

Vilcsek, E., and H. Wänke, Das Strahlungsalter der Eisenmeteorite aus Chlor-36-Messungen, *Z. Naturforsch., 16a,* 379–384, 1961.

Vilcsek, E., and H. Wänke, Cosmic ray exposure ages and terrestrial ages of stone and iron meteorites derived from chlorine-36 and argon-39 measurements, in *Radioactive Dating,* pp. 381–393, International Atomic Energy Agency, Vienna, 1963.

Voshage, H., and D. C. Hess, Strahlungsalter einiger Eisenmeteorite, *Z. Naturforsch., 19a,* 341–346, 1964.

(Manuscript received April 6, 1965; revised August 31, 1965.)